Laser and Particle Beams (2004), *22*, 323–333. Printed in the USA.

DOI: 10.1017/S0263034604223175

An ensemble of new techniques to study soft-X-ray-induced variations in cellular metabolism

EDMOND TURCU,[1] RICK ALLOT,[1] NICOLA LISI,[1] DIMITRI BATANI,[2] FULVIA BORTOLOTTO,[2] ALESSANDRA MASINI,[2] MARZIALE MILANI,[3] MONICA BALLERINI,[3] LORENZO FERRARO,[3] ACHILLE POZZI,[3] FABIO PREVIDI,[4] AND LORENZO REBONATO[4]

[1]Rutherford Appleton Laboratory, Chilton Didcot, UK
[2]Dipartimento di Fisica, "G.Occhialini," Università degli Studi di Milano–Bicocca, and INFM, Milano, Italy
[3]Dipartimento di Scienza dei Materiali, Università degli Studi di Milano–Bicocca, and INFM, Milano, Italy
[4]Dipartimento di Elettronica e Informazione, Politecnico di Milano, Milano, Italy

(RECEIVED 1 November 2003; ACCEPTED 26 January 2004)

Abstract

An ensemble of new techniques has been developed to study cell metabolism. These include: CO_2 production monitoring, cell irradiation with soft X rays produced with a laser-plasma source, and study of oscillations in cell metabolic activity via spectral analysis of experimental records. Soft X-rays at about 0.9 keV, with a very low penetration in biological material, were chosen to produce damages at the metabolic level, without great interference with DNA activity. The use of a laser-plasma source allowed a fast deposition of high doses. Monitoring of CO_2 production allowed us to measure cell metabolic response immediately after irradiation in a continuous and noninvasive way. Also a simple model was developed to calculate X-ray doses delivered to the different cell compartments following a Lambert–Bouguet–Beer law. Results obtained on *Saccharomyces cerevisiae* yeast cells in experiments performed at Rutherford Appleton Laboratory are presented.

Keywords: Laser plasmas; Metabolism; Radiobiology; Soft X-rays; X-ray dosimetry; X-ray spectroscopy; Yeast

1. INTRODUCTION

The study of the interaction of biological cells with ionizing radiation is very important in biophysics and medical physics in order to investigate cell behavior and cell response to external factors and to understand how cells are working even in normal conditions. In respect to this, the recent advent of high-brightness X-ray sources, like synchrotrons and laser-plasma sources, has implied important changes in experimental techniques. Indeed, unlike conventional sources, which require long exposure times to give high irradiation doses, such sources allow a very fast deposition of high doses. Hence the damage can be considered to take place almost instantaneously, and the cell reaction begins immediately after the damage. This allows a clear separation of the two steps of dose deposition and repair, which may not be the case with low brightness sources, and hence allows the realization of conceptually cleaner experiments.

Also laser-plasma sources are very efficient in the low energy part of the X-ray spectrum, allowing new wavelengths to be used in radiobiology experiments. As already pointed out in literature, these wavelengths are interesting not only because of an increase in the range of investigated parameters, but also because the low photon energy implies low energy secondary electrons and hence damage that is strictly localized around the deposition region (Con *et al.*, 1977; Goodhead, 1977; Goodhead & Thacker, 1977). In the case of the experiments that will be presented in this article, another important characteristic of low energy X-ray photons has been exploited, namely, that they may have a very short penetration range in biological matter. Thus, by carefully choosing the irradiation wavelength, it is, in principle, conceivable to perform differential experiments in radiobiology, realizing a preferential dose deposition to the external cell compartments (cell membrane and cytoplasm) with little interference with DNA genetic activity taking place in the cell nucleus. This is important because such external

Address correspondence and reprint requests to: Dmitri Batani, Dipartimento di Fisica, "G. Occhialini," Università degli Studi di Milano-Bicocca, and INFM, Piazza della Scienza 3, 20126 Milano, Italy. E-mail: batani@mib.infn.it

compartments are strictly related to the cell metabolic activity, which is the subject of the techniques presented in this article.

In our experiments, a laser-plasma source has been used to irradiate *Saccharomyces cerevisiae* yeast cells with soft X-rays. The experiment has been realized at Rutherford Appleton Laboratory with the goal of affecting and studying cell metabolism (Turcu *et al.*, 1994*a*, 1994*b*). Yeast cells have largely been used as a model system for investigating cellular metabolic activity, in particular because they are eukaryotic cells, hence strictly related to higher organisms, while at the same time being relatively simple and unicellular (Tuite, 1964; Fremter, 1983). Moreover they are easy to handle, nonpathogenic, and can be dehydrated and stay viable.

Teflon (CF_2) strips were used as the laser target (Batani *et al.*, 1995, 1996), emitting a *K*-shell X-ray spectrum from *F* ions centered on 0.9 keV, with a very large absorption in biological matter. The structure of yeast, characterized by a large and massive cell wall (Klis, 1994; Batani *et al.*, 1998) contributed to stopping the X-rays before the nucleus, supporting the idea of inducing differential damages.

To verify the occurrence of such preferential energy deposition, X-ray doses to the different cell regions were calculated following the exponential Lambert–Bouguet–Beer law through a spherical model of the cell with concentric and differentiated compartments.

The use of high-brightness sources and low-energy X rays might, however, be of limited use if it is not coupled to new investigation diagnostic means. Indeed the classical techniques used in radiobiology experiments to monitor cell response, in particular the colony's formation ability, necessarily imply a measurement of cellular response at very late times. Moreover, only those damages capable of an influence on daughter cells, that is, on following generations, are registered, which again restricts the investigation to damages of a genetic nature. When metabolic activity is investigated, other diagnostics must then be developed.

In our case the experimental technique is based on monitoring the production of CO_2 from the cells with pressure sensors. This is an old technique (Warburg, 1930), which may now be rediscovered, taking advantage of recent technological developments. The analysis can start immediately after irradiation and can be continued up to several hours. Other advantages are that the technique is on-line and noninvasive, preserves the cell population, and can give quantitative information in a continuous way. Also it allows us to monitor the response of cells to external perturbations. In the present study such perturbations have been induced by changes in the feeding conditions (type of sugar) and/or by soft X-ray irradiation.

The study of CO_2 production is interesting because it is related to energy production (through the glycolytic cycle and the ATP–ADP balance), being one of the final products of metabolic activity. There is a complicated series of enzymatic reactions for the degradation of sugar, which, in eukaryotic cells, includes respiration, in the presence of oxygen, and fermentation, for instance in yeast cells, in anaerobic conditions.

Metabolic oscillations in yeast have been evidenced and appear to be a relevant tool for the investigation of control and feedback mechanisms at work in biological systems (Nicolis & Prigogine, 1977; Winfree, 1983; Cortassa & Aon, 1994). Here, to evidence their presence, the obtained experimental records of pressure versus time were analyzed with a spectral technique based on the discrete Fourier transform (DFT) algorithm (Brillinger, 1981; Ljung, 1987). Oscillations were indeed observed and it was shown that soft X-ray irradiation changed their period. Unlike other approaches already used in literature, our technique not only is, again, noninvasive, but allows metabolic oscillations to be evidenced in a whole cell population.

In this article, after describing in detail the different parts of the experimental setup, some preliminary experimental results are shown. Although some aspects of the several techniques described in this article have already been, partially, presented in literature, we think that the combined approach presented here fully exploits their potentials, and may finally lead to the development of new experimental techniques in radiobiology.

2. PREPARATION OF THE BIOLOGICAL SAMPLES

The biological specimen was commercial dry *Saccharomyces cerevisiae Hansen* yeast (produced by Aboca) that needed to be hydrated about 1 h before use. The analyzed samples were fixed volumes (4 ml) of a suspension of cells in deionized water (or phosphate buffer) with a typical concentration of 2 mg/ml corresponding to about 2×10^7 cells/ml. The cells were deposited on a paper filter in a monolayer by filtering in a Venturi tube. The used filters were Whatman standard cellulose filter papers of grade 1.

After a short period for drying, the filters were put onto a Hostaphan film so that yeast cells were hosted by a "sandwich" made of Hostaphan on one side and paper filter on the other. The thickness of the Hostaphan filter was 1 μm.

For the samples undergoing irradiation, such sandwiches were then deposited into an automatic handling robot for X-ray exposure (the Hostaphan film facing the X-ray source) and the dose could be delivered. Finally the filters were put again in the same quantity of water (4 ml) and the bottles were sealed and submerged in a thermal bath at 32°C (temperature variations were lower than 0.1°C). Different kinds of sugar were added to the suspension as nourishment in order to study the different metabolic responses. The standard sugar concentration was 20 mg/ml.

Some intermediate investigations were performed, including the optimization of the support of the biological target (trying different paper filters and different preparation procedures). We also verified that CO_2 production from simple cell suspensions was equivalent to that of sample deposited

https://doi.org/10.1017/S0263034604223175 Published online by Cambridge University Press

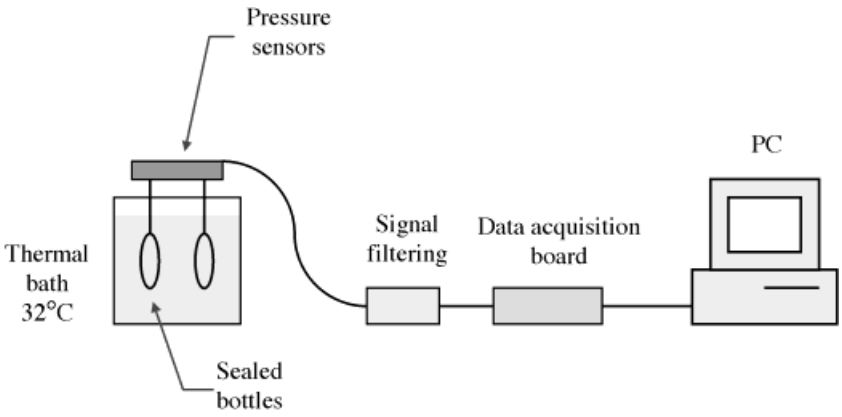

Fig. 1. Acquisition system of the Miteco Low Pressure Sensor type AM5310 DV.

on the paper filters. To study specifically fermentation, during some experimental runs an Argon atmosphere was used instead of air normally present in the bottle, in order to realize more strict anaerobic conditions and cause a complete inhibition of respiration.

3. GAS PRODUCTION MEASUREMENT

The overall process is based on the measurement of the pressure increase in sealed bottles where CO_2 production can be monitored. The bottles were connected to the pressure sensors whose output is linked to a PC through an Amplicon 16-bit 20 K sample/s data acquisition board, which has a resolution less than 1.5 μV.

The pressure sensors were connected to a stabilized 10 V power supply. We used differential silicon pressure sensors (Low Pressure Sensor type AM5310 DV from Miteco) of high sensitivity (from 0 to 100 mbar, giving 25-mV full-scale output, with an estimated accuracy of 0.1 mV and a sensitivity of about 2.5 mbar/mV). Figure 1 shows the scheme of the data acquisition system.

The sensors were calibrated, showing a very good linearity in the region of interest (0–100 mbar) and further on. Also no hysteresis was observed (Batani *et al.*, 1995; Costato *et al.*, 1996).

Before analyzing the data, we verified that for control samples (pure water) the pressure measurements precisely reflected the atmospheric pressure behavior. Also, to be sure that the pressure increase was really due to CO_2 production, mass spectrometry was used. Figure 2 shows that the gas produced during fermentation is CO_2 (mass number 44) that was not present in the initial blank run.

The acquisition system allowed the simultaneous recording of data from 16 different sample bottles. To check data reproducibility we always had different runs for the same parameters.

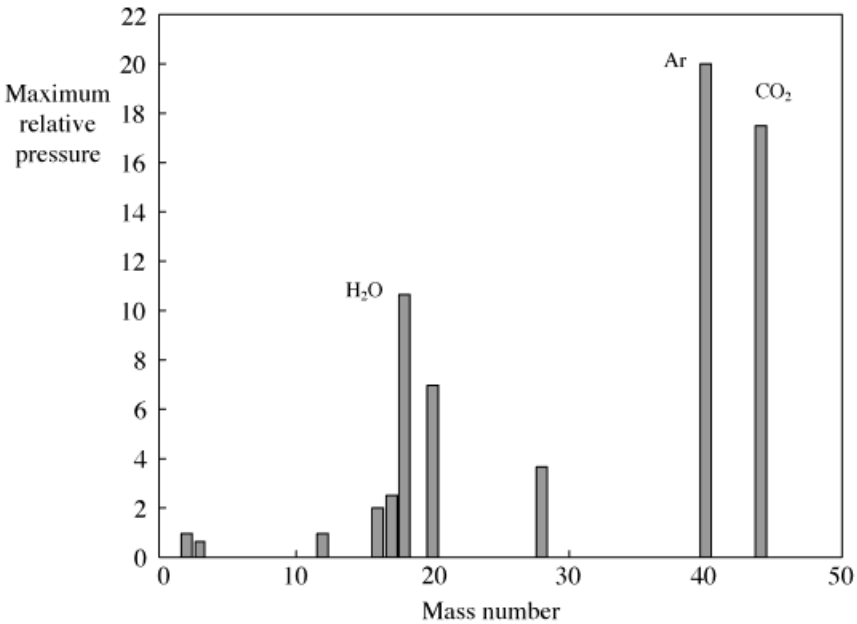

Fig. 2. Mass spectrometry of produced gas as a function of mass number. The initial atmosphere was argon only, corresponding to anaerobic conditions. The gas produced during fermentation is CO_2 (mass number 44) that was not present in the initial blank run.

https://doi.org/10.1017/S0263034604223175 Published online by Cambridge University Press

4. THE RADIATION SOURCE

The source was obtained with a complex laser system. A Nd laser, converted to 2ω, was used to pump a dye oscillator followed by dye amplifiers (pumped by an excimer laser) and by frequency converter crystals. The laser pulse so obtained was transformed by spatial and temporal multiplexing in a train of pulses (each 7 ps long), which underwent a final large amplification in KrF amplifiers, producing UV radiation at $\lambda = 248$ nm. Such laser radiation was focused onto the target with a $f = 9$ cm focusing lens producing an intensity of the order of 5×10^{15} W/cm^2. The overall system is very similar to the one already described by Turcu *et al.* (1994*a*, 1994*b*).

A relevant element for the success of the experiment was the availability of a computer driven robot for sample exposure and of a dose control system. The exposure robot was developed at Rutherford Appleton Laboratory to irradiate mammal cells with Cu *L*-shell X-rays (Turcu *et al.*, 1994*a*, 1994*b*).

The dose control system was based on a silicon PIN diode that measured the X-ray energy produced by each pulse. The PIN was just beside the cell samples and had the same filters placed before the cells to exactly measure the same radiation that biological samples were exposed to. Because a single laser shot was, in general, not enough to give the required dose, successive PIN signals were integrated and summed until the required dose was delivered. The computer then automatically stopped the laser, also giving the number of laser shots and the histogram of the dose distribution. In a few minutes the irradiation procedure was completed. Figure 3 shows the scheme of the irradiation procedure.

The soft X-ray spectrum was also registered (see Section 4), which allowed an absolute calibration of the PIN diode response. The conversion factor used to transform the integrated PIN diode signal (corresponding to a collected electrical charge (in nanocoulombs) to an absorbed dose (in radians) was 2.6 rad/nC at 0.9 keV. This factor is dependent on photon energy because of the variation of PIN sensitivity and the different photon penetration into the biological material.

5. SPECTRAL CHARACTERIZATION OF THE SOFT X-RAY SOURCE

The X-ray spectral region, which can be used for the purpose of producing preferential damage in the cell external compartments, is quite narrow. It was known that X rays with $h\nu \approx 1.2$ keV, already used for DNA recovery experiments, are characterized by a large penetration depth in undifferentiated biological material ($\approx 5\ \mu$m) and hence can deposit a large quantity of their energy into the cell nucleus (Turcu *et al.*, 1994*a*, 1994*b*). On the other side, the attenuation coefficient is also low for X rays in the "water window" region (300–500 eV) as shown in Figure 4.

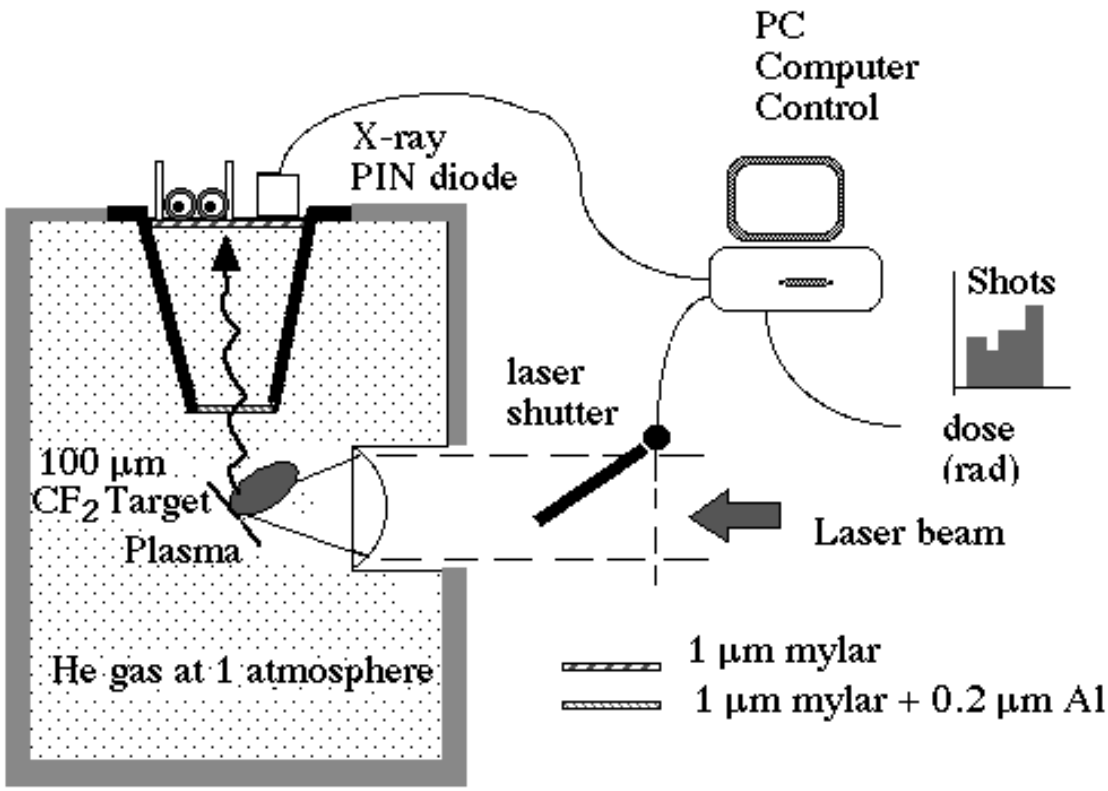

Fig. 3. Scheme of the irradiation procedure.

https://doi.org/10.1017/S0263034604223175 Published online by Cambridge University Press

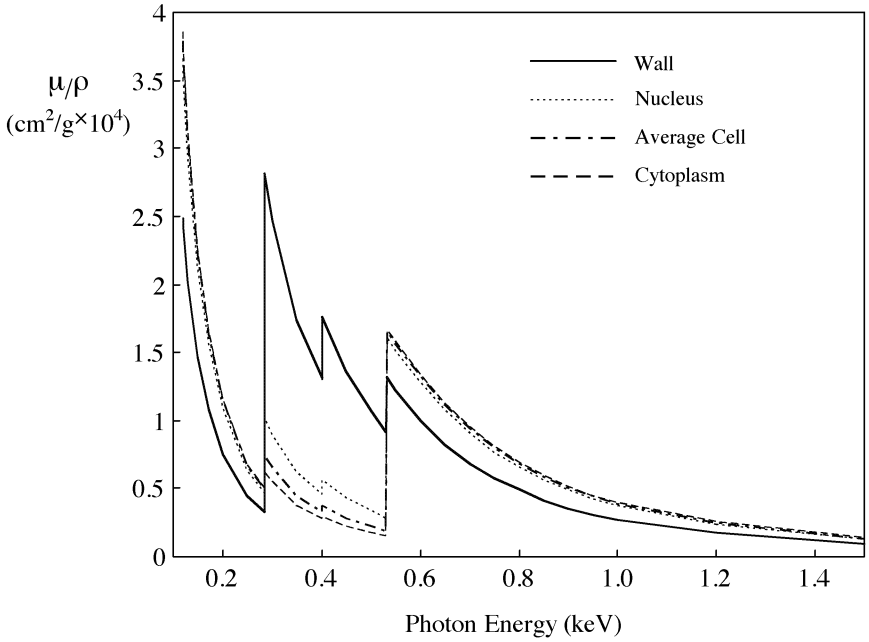

Fig. 4. Mass absorption coefficient (μ/ρ in $cm^2/g \times 10^4$) of biological material (wall) and biological material with various percentages of water (corresponding to cytoplasm, nucleus, average cell) versus photon energy in kiloelectron volts.

The target material should then be chosen to give emission at energies as close as possible to the end of water window (corresponding to the O-absorption edge). Also a *K*-shell spectrum, characterized by only a few lines, would be preferable, making the dose calculations much easier. Unfortunately there are not many elements with these characteristics. We chose fluorine, or rather Teflon (CF_2), which was produced in thin strips (100 μm thick). The use of strips drastically reduces the emission of debris, which could damage the optics and/or the biological samples (Bijkerk *et al.*, 1992). Unfortunately, CF_2 tapes also contain carbon, which emits exactly in the water window. In the present experiment, such undesired *K*-shell C emission has been removed by putting appropriate filters (2 μm mylar plus 0.2 μm Al) before the biological samples; these filters also removed scattered UV laser light, which could produce important biological effects. An additional gas buffer (He at 1 atmosphere) was present in the interaction chamber with the main role of further reducing debris effects, but also contributing to stop softer carbon emission.

In the observed wavelength range, fluorine emits a *K*-shell X-ray spectrum (comprised between the fluorine He-α at 731 eV and the ionization edge for the H-like ion at 1103 eV). The spectra were recorded with flat crystal minispectrometers (described in Batani *et al.*, 1991) using RbAP crystals ($2d = 26.121$ Å) and Kodak DEF film and filtered with 2 μm mylar and 0.2 μm Al. While recording some spectra, a Cu layer was also added on half the slit: Because Cu is characterized by the *L*-absorption edge at $h\nu \approx 0.993$ keV, this gave a wavelength fiducial on the film, which was useful for spectra interpretation. Densitometries of the spectra (see Fig. 5) were obtained with a Joyce Laoebl 3CS Microdensitometer at RAL. Absolute X-ray intensities were calculated taking into account film sensitivity (Rockett *et al.*, 1985), filter and buffer gas transparency (Henke, 1986), and crystal reflectivity (Alexandropoulus & Cohen, 1974).

6. DOSIMETRY

The information on cell morphology and the analysis of the X-ray spectrum allow the development of a detailed spherical model of the cell for the evaluation of the energy absorbed by each compartment of the microorganism. We recall that, in a previous work (Batani *et al.*, 1998) the following quantities were measured for the yeast used in this experiment: cell average radius $r_0 = 2.58 \pm 0.54$ μm, total membrane and wall thickness 0.18 ± 0.02 μm, nucleus radius $r_n = 0.95 \pm 0.12$ μm. Also their distribution across the cellular population was measured.

The model allows us to separately calculate the doses in the main cell compartments (wall, cytoplasm, nucleus, considered spherical and concentric) and to draw a picture of where X-rays are absorbed and radiation effects are more likely to occur. This is clear progress with respect to the approach normally used in cellular radiobiology (see, e.g., Frankenberg *et al.*, 1986) in which only the radiation penetration depth in the undifferentiated biological material and the average dose to the whole cell are considered (in our case, $h\nu \approx 0.9$ keV, the penetration depth in an undifferentiated average cell, made of 90% water, is about 1.86 μm).

The absorption coefficients and densities of the three cell compartments are computed according to the following rationale:

1. The wall is made of undifferentiated biological material (with no water) with 7% hydrogen, 22.5% oxygen, 52% carbon, 16.5% nitrogen, 1.5% sulphur in weight

https://doi.org/10.1017/S0263034604223175 Published online by Cambridge University Press

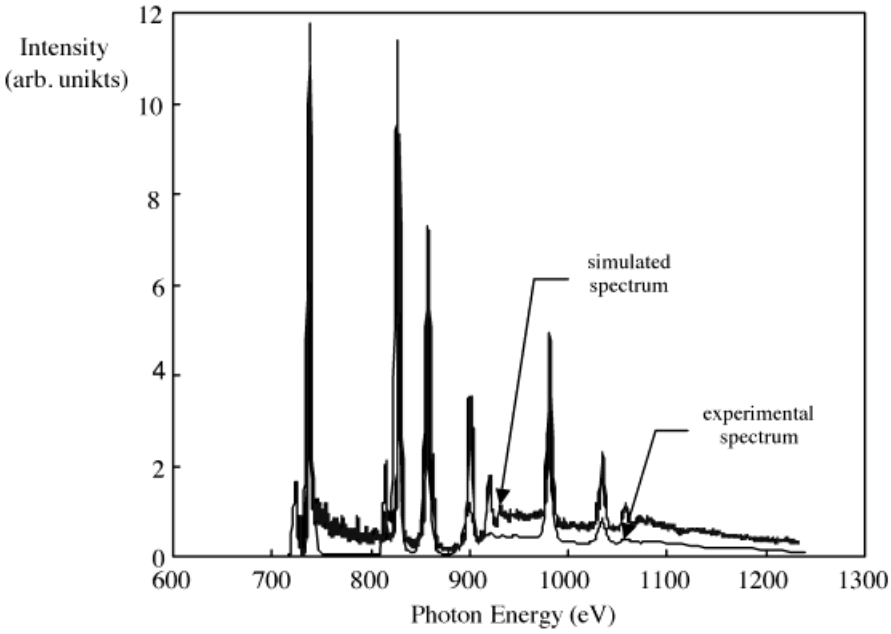

Fig. 5. Experimental deconvoluted Teflon spectrum recorded on Kodak DEF film and corresponding simulated spectrum. Densitometry obtained with a Joyce Laoebl 3CS Microdensitometer.

(as deduced from Frankenberg *et al*., 1986; Weast & Astle, 1983) with a $\rho = 1.6118$ g/cm^3 average density;
2. The cytoplasm is composed of 95% water and 5% biological material, with a $\rho = 1.0306$ g/cm^3 average density;
3. The nucleus is made of 78% water and 22% biological material, with a $\rho = 1.135$ g/cm^3 average density.

The cell average density is $\rho = 1.06118$ g/cm^3 (90% water), comparable to the value (1.08 g/cm^3) reported by Frankenberg *et al*. (1986).

In the numerical model, cylindrical coordinates are used and the cell is divided into a series of elemental volumes in each of which the absorbed doses is numerically computed using the Lambert–Bouguet–Beer law, that is, the X-ray energy dE absorbed by a layer with thickness dx, surface A, density ρ, and absorption coefficient μ is given by

$$dE = I(h\nu x)A\rho\mu dx. \tag{1}$$

Here $I(h\nu, x)$ is the X-ray flux of photons with energy $h\nu$ at position x. Hence $I(h\nu,0)$ is the spectrum emitted from the plasma, and, to calculate $I(h\nu, x)$ it is necessary to consider the various filters in front of the biological samples (0.2 μm Al and 2 μm mylar), their transparency, that of helium, and that of the biological material itself. The doses absorbed are then computed by summing over the elemental volumes in each compartment. To assure the precision of the numerical calculus, the difference between the smallest compartment volume and the sum of all the elemental volumes inside it is taken to be smaller than a precision parameter fixed *a priori*. Also, in the case of a homogenous spherical cell, an analytical solution can be found which gives the same result of the finite element calculations.

In this way it is possible to perform a simple study of the influence of the various parameters (compartment sizes, cell composition, radiation wavelength) on the absorbed dose.

Figure 6 shows the calculated doses for two values of the X-ray energy for a cell with average dimension of the three compartments. "Our" 0.9-keV radiation is compared to 1.5-keV soft X-rays, which would be obtained by focusing the laser onto an Al target (Turcu *et al.*, 1994*a*, 1994*b*), corresponding to Al *K*-shell emission. The harder radiation is characterized by a much bigger energy deposition to the cell nucleus. Moreover, the ratio between the dose to the wall and the dose to the nucleus is higher for the softer radiation.

To take into account the variation of the absorbed doses due to the different sizes of the cells, calculations were performed for various values of the cell radius. In particular, Figure 7 shows the doses to wall, cytoplasm, and nucleus for different cell sizes. It is clear how the dose absorbed by the nucleus is higher in cells with a 2-μm radius, which are likely to be found in the real cell suspension.

7. SPECTRAL ANALYSIS OF CO_2 PRODUCTION VERSUS TIME

Often, after 2–3 h, oscillations became evident in CO_2 production in many samples. We then performed a spectral analysis of these time series to extract the principal harmonic component of the signal.

It is well known (Brillinger, 1981; Ljung, 1987) that, given a sampled signal $\{s(t)\}_{t=1,\ldots N}$ an estimate of its Fourier transform is given by

$$S_N(\omega) = \frac{1}{\sqrt{N}} \sum_{t=1}^{N} s(t)e^{-j\omega t}. \tag{2}$$

https://doi.org/10.1017/S0263034604223175 Published online by Cambridge University Press

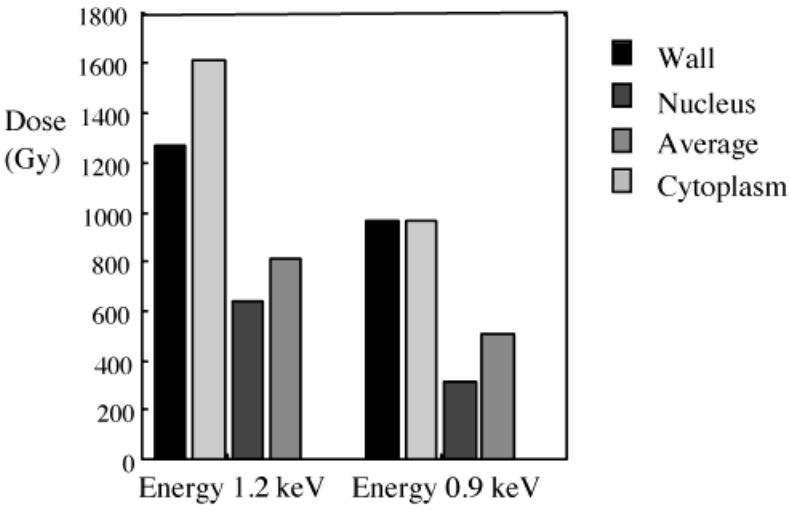

Fig. 6. Results of cell dosimetry for two values of X-ray energy: 0.9 keV, corresponding to Teflon emission, and 1.5 keV, corresponding to Al *K*-shell emission. The wall thickness is 200 nm. Doses are in grays and they are calculated assuming an X-ray flux equal to 1 mJ/cm^2 before the filters.

It can be proved that the estimate in Eq. (2) is asymptotically (for $N \to \infty$) unbiased but its variance does not decrease as N increases. So a smoothing procedure has been used, which is the only way to improve the poor variance properties of this estimator. In this way a modification of Eq. (2) is obtained through convolution with a smooth function of time whose Fourier transform is frequency window $W\gamma(\omega)$, which has the property to be sufficiently narrow to give relevance to a small group of frequencies at a time, while estimation occurs. In particular a Bartlett window has been used:

$$W\gamma(\omega) = \frac{1}{\gamma}\left(\frac{\sin\left(\frac{\gamma\omega}{2}\right)}{\sin\left(\frac{\omega}{2}\right)}\right)^2. \qquad (3)$$

The parameter γ indicates how large the window is: as γ increases the frequency window gets narrower.

The choice of the parameter γ is critical; some procedures for optimal estimates of the window width in transfer function estimation are given by Brillinger (1981) and Ljung (1987), but they need knowledge of quantities usually not available in the practical applications, such as the spectrum of the noise affecting the measurement. So, in this case, a practical procedure (Ljung, 1987) to solve the bias-variance trade-off has been used: First initialize the parameter γ at $\gamma \cong N/20$, where N is the number of available data; then compute and plot the Fourier transform estimate for increasing values of γ; as γ increases, more details of the transform appear, initially due to bias decrease and, from a certain value of γ on, due to variance increment. The user should choose the value of γ that he feels will separate the two phenomena.

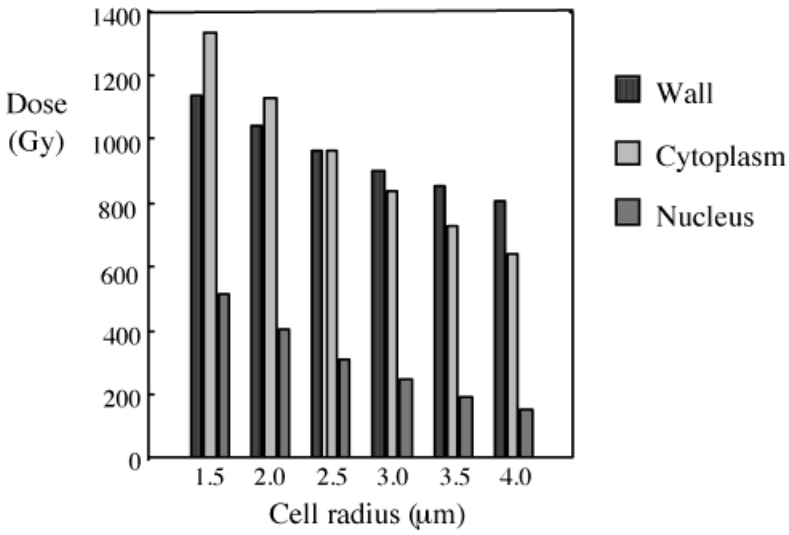

Fig. 7. Dosimetry of yeast cells as a function of cell radius calculated for 0.9 keV X-ray radiation and assuming an X-ray flux equal to 1 mJ/cm^2 before the filters. Wall thickness and nuclear radius are assumed to change in a constant ratio with the cell radius.

https://doi.org/10.1017/S0263034604223175 Published online by Cambridge University Press

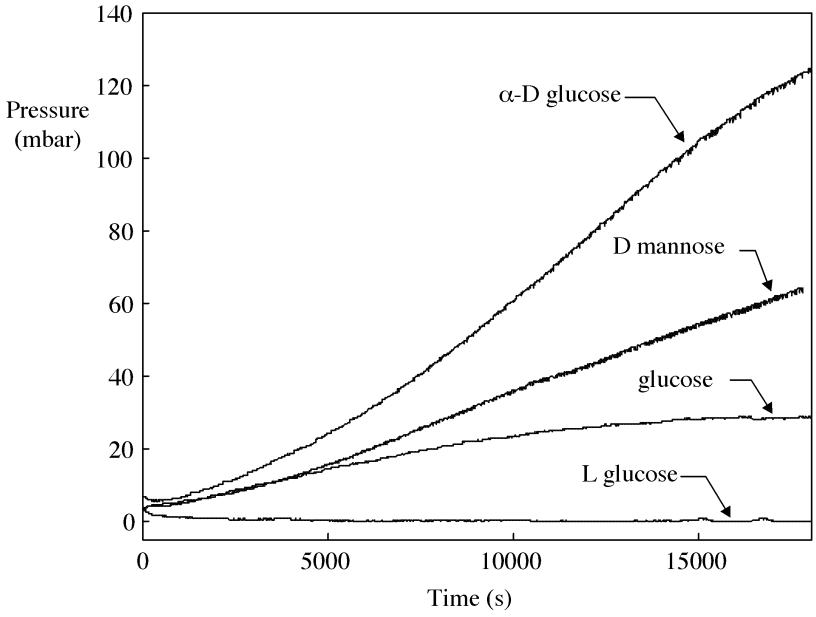

Fig. 8. CO_2 pressure measurements for samples fed with different kinds of sugars, that is, L-glucose, glucose, D-mannose, and αD-glucose.

8. PRELIMINARY RESULTS

CO_2 production was monitored by pressure silicon detectors with both irradiated and nonirradiated samples. First, we analyzed in detail CO_2 production versus time on a very large amount of nonirradiated samples. Figure 8 shows the effects of the different sugars used in the sample suspensions on the cell metabolic activity, which can be easily evidenced with our monitoring technique. The different rate of pressure increase shows the different cell capability of assuming different nutrients, that is, L-glucose, glucose, D-mannose, and αD-glucose. In particular, no CO_2 pressure increase is visible for samples fed with L-glucose, which has a chirality that does not allow this sugar to be metabolized. This analysis has been performed to show that an accurate CO_2 pressure measurement is an efficient tool for the study of cell metabolic activity; moreover it is affordable, precise, and reproducible.

Concerning oscillations, for the nonirradiated sample of Figure 9, a principal frequency component corresponding to a period of 35.7 ± 2.5 s is clearly visible. A very similar estimate of the oscillation period has been obtained from

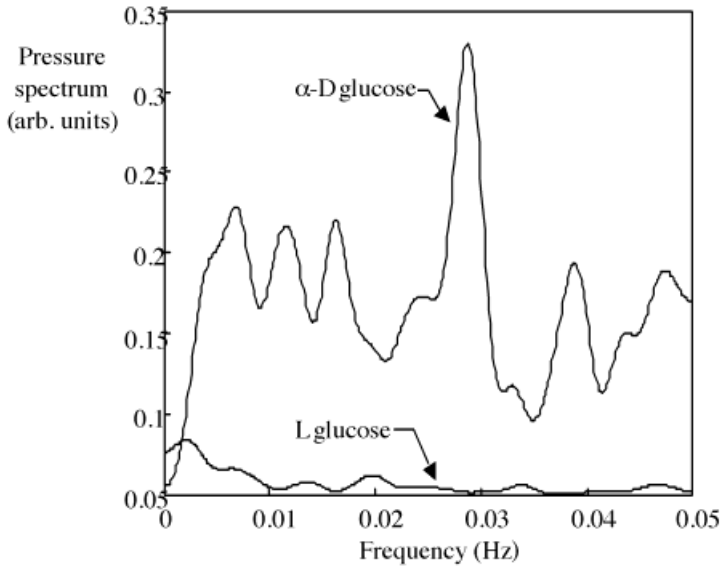

Fig. 9. Typical power spectra for a sample of standard cell suspension with αD-glucose. A principal frequency of 35.7 ± 2.5 s is visible. Comparison with a suspension fed with L-glucose is also shown.

https://doi.org/10.1017/S0263034604223175 Published online by Cambridge University Press

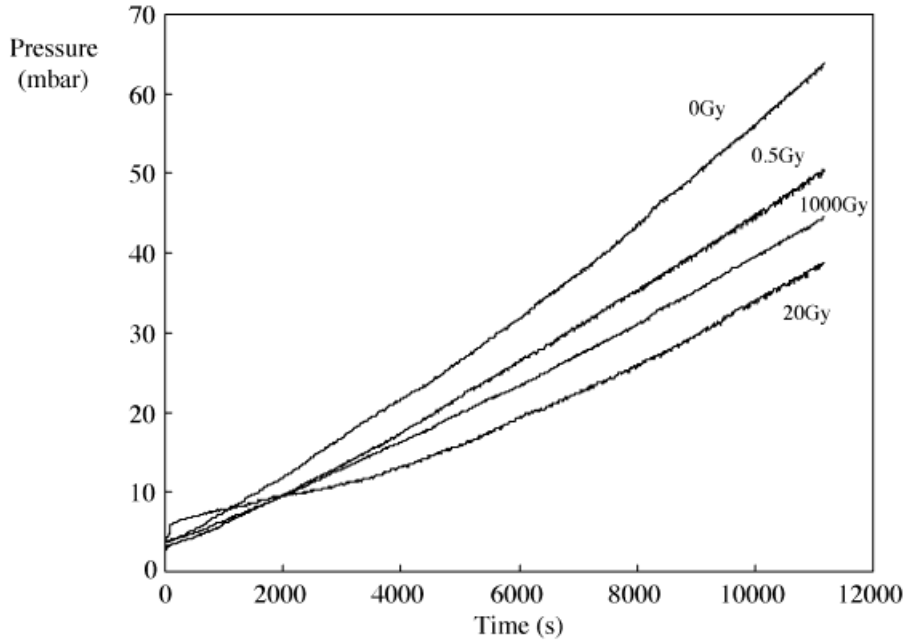

Fig. 10. Effect on CO_2 production of irradiation. Comparison between the power spectra of a nonirradiated cell suspension and a 20 Gy irradiated one; αD-glucose was used as nourishment in both suspensions.

different samples; in all cases the considered samples were 4 ml of a suspension with 20 mg/ml of αD-glucose and 2 mg/ml of yeast. Such oscillations were not found in the simultaneously analyzed control water. The evidence of their metabolic origin is also confirmed by the analysis of yeast cell suspension fed with L-glucose, in which we never observed any oscillatory phenomenon (see Fig. 9). The fact that oscillations are not found in the control water, and their amplitude is much larger than the sensor sensitivity, reasonably implies that we are not facing ghosts or experimental artifacts.

For the irradiated samples (doses between 0.5 and 1000 Gy) oscillations were also observed. All the samples were fed with αD-glucose, which enhanced the metabolic response. Figure 10 shows the frequency shifting and mixing as a consequence of irradiation for cells exposed with 20 Gy. The main frequency peak is shifted toward lower frequencies (giving now a main component period of 52.6 ± 5.5 s) and the rising of other frequency components is clearly visible. Such perturbations of spectra with frequency shifts and the appearance of new frequency components were registered in all the irradiated samples, which exhibited oscillations. Anyway whereas a period of about 36 s has been observed as greatly dominant in most nonirradiated samples, in the case of irradiated cells no clear correlation between X-ray dose and the profile of the spectrum has been found for the moment. However, in general, because the main harmonic component moves toward lower frequencies, the metabolism of irradiated cells appears to occur at slightly lower rates, as confirmed also by the observed slower increase in CO_2 pressure. The appearance of many frequencies could possibly be linked to the activation or exaltation of some less important glycolytic reactions, as already observed by Hesse (1979).

Finally, Figure 11a, b shows the variation of pressure as a function of time for a suspension after irradiation with soft X-rays from Cu and CF_2 targets. The scales on the two figures are the same, showing how the effect is larger for irradiation with the softer and less penetrating CF_2 X-rays. This confirms that radiation is absorbed at different depths in the cell and produces different metabolic effects. Again a nonmonotonic response versus X-ray dose is evidenced in both figures.

9. CONCLUSIONS

Oscillations related to metabolism have been previously observed in yeast extract (Aon *et al.*, 1992) and in single yeast cells (Betz, 1968; Boiteux *et al.*, 1975) with other very invasive techniques. Because we observe the phenomenon in yeast cell populations, a synchronization mechanism must take place, which correlates the different cells and phases them. Such mechanisms have already been described in literature as shock synchronization and starvation synchronization (Cameron & Padilla, 1966; Kockova-Kratochvilova, 1990; Tuite & Oliver, 1991; Chance *et al.*, 1964).

Concerning CO_2 production rate versus irradiation dose, we observed (Batani *et al.*, 1995, 1996) a nonlinear and nonmonotonic behavior, which is quite different from what is usually found in radiobiology experiments. The usual approach (e.g., see Tuite & Oliver, 1991; Turcu *et al.*, 1994*a*,

https://doi.org/10.1017/S0263034604223175 Published online by Cambridge University Press

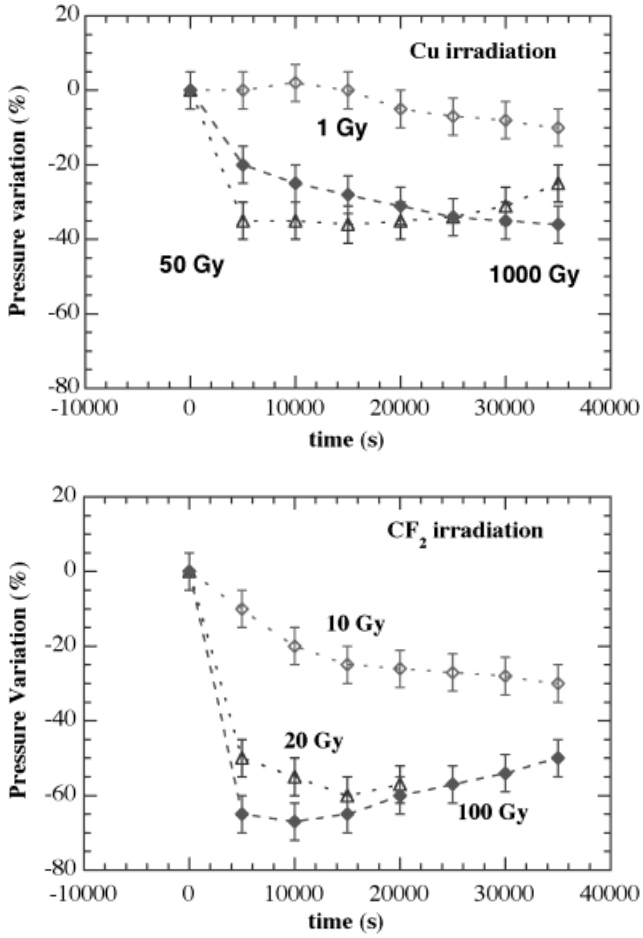

Fig. 11. Variation of pressure (with respect to nonirradiated cells) as a function of time after irradiation with soft X-rays from Cu (a) and CF_2 (b) targets. The effect is larger for irradiation with the softer and less penetrating CF_2 X rays. Also, a nonmonotonic response versus X-ray dose is evidenced in both figures.

1994*b*) is based on the study of survival curves, that is the capability of individual cells to develop colonies after the damage induced by X rays. This only gives the response at very long times after irradiation, thereby losing all the information on fast cell response to damages and about cell damages that are not likely to be transmitted to the genetic descendants.

The highlighting of such early responses is possible thanks to the use of CO_2 monitoring as a technique to follow cell metabolism and to the use of a high-brightness laser-plasma X-ray source that allows us to deliver large doses in a short time. This implies that cell reaction to the damaging factors does not start before the complete dose deposition: Hence there are not changes in the biophysics of the studied process during the deposition phase, as frequently happens in cell radiobiology.

These are only some examples of the sensitivity and reliability of the diagnostics technique we have developed. Such encouraging results may be applied to other types of cells in different experiments and may hence be of general importance to radiobiology and biophysics studies.

ACKNOWLEDGMENTS

The experiment has been realized at the Rutherford Appleton Laboratory and fully supported by the E.U. Human Capital and Mobility "Large Scale Facilities Access" Programme. We also acknowledge a contribution from INFM, CNR (contract n. 96.00266.CT02.115.27689), and NATO (grant n. GRC961133). The authors are indebted to D. Stevens and M. Hill (Medical Research Council, Harwell) for stimulating discussions and technical support. A. Pozzi thanks the Italian Physical Society (SIF) and A. Masini the INFM for their grants. Special thanks are due to Cyril Brown, Anthony Parker, Colin Danson, Chris Edwards, Nick Allen, Katherine Hale, Irene Gray, Sue Tavender, William Toner of RAL, and to Franco Cotelli and Carla Lora Lamia of Dipartimento di Scienze Biologiche (Milano). Finally we would like to recall the memory of Prof. Michele Costato, who was the main initiator of this work.

REFERENCES

Alexandropoulus, N.G. & Cohen, G.G. (1974). *Appl. Spectr.* **28**, 2.

Aon, M.A., Cortassa, S., Westerhoff, H.V. & Van Dam, K. (1992). *J. Gen. Microbiol.,* **138**.

Batani, D., Masini, A., Milani, M., *et al.* (1996). *Il Nuovo Cimento* **18D**, 657.

Batani, D., Milani, M., Masini, A., Pozzi, A., Costato, M., Turcu, E., Lisi, N., Allot, R., Lora Lamia Donin, C., Cotelli, F., Previdi, F., Faral, B., Conte, E., Moret, M. & Poletti, G. (1998). Characterisation of *Saccharomyces cerevisiae* yeast cells. *Physica Medica* **15**, 151–157.

Batani, D., Milani, M., Masini, A., Previdi, F., Turcu, E., *et al.* (1995). *Laser Technol.* **5**, 3.

Batani, D., Turcu, E., Tallents, G.J., Giulietti, A. & Palladino, L. (1991). *SPIE Proc.* **1503**, 479.

Betz, A. (1968). In *Quantitative Biology and Metabolism*. (Locker, A., Ed.). Springer-Verlag.

Bijkerk, F., Louis, E., Van der Wiel, M., Turcu, E., Tallents, G.J. & Batani, D. (1992). *J. X-ray Sci. Tech.* **3**, 133.

Boiteux, A., Goldbeter, A. & Hesse, B. (1975). *Proc. Natl. Acad. Sci., USA* **72**, 1975.

Brillinger, D.R. (1981). Time Series: Data Analysis and Theory. San Francisco: Holden-Day.

Cameron, I.L. & Padilla, G.M. (1966). *Cell Synchrony*. New York: Academic Press.

Chance, B., Estabrook, R.W. & Ghosh, A. (1964). *Proc. Natl. Acad. Sci., USA* **51**, 1964.

Con, R., Thacker, J. & Goodhead, D. (1977). *Int. J. Radiat. Biol.* **31**, 561.

Cortassa, S. & Aon, M.A. (1994). *Cell Biol. Int.* **18**, 687.

Costato, M., Masini, A., Michelini, A., Milani, M. & Pozzi, A. (1996). *Laser Technol.* **6**, 85.

Frankenberg, D. & Goodhead, D.T., *et al.* (1986). *Int. J. Radiat. Biol.* **50**, 727.

Fremter, E. (1983). In *Biophysics* (Hoppe, W. *et al.*, Eds.). Berlin: Springer-Verlag.

Goodhead, D. (1977). *Int. J. Radiat. Biol.* **32**, 43.

Goodhead, D. & Thacker, J. (1977). *Int. J. Radiat. Biol.* **31**, 541.

Henke, B.L. (1986). In *X-ray Data Booklet*. (Vaughan, D., Ed.). Berkeley, CA: Center for X-ray optics.

Hesse, B. (1979). *J. Exp. Biol.* **81**.

https://doi.org/10.1017/S0263034604223175 Published online by Cambridge University Press

Klis, F.M. (1994). *Yeast* **10**, 851.
Kockova-Kratochvilova, A. (1990). *Yeast and Yeast-like Organisms*. New York and Weinheim: VCH.
Ljung, L. (1987). System Identification: Theory for the User. Englewood Cliffs, NJ: Prentice-Hall.
Nicolis, G. & Prigogine, I. (1977). *Self Organisation in Non Equilibrium Systems from Dissipative Structures to Order through Fluctuations*. New York: Wiley & Sons Inc.
Rockett, P.D., Bird, C.R., Hailey, C.J., Sullivan, D., Brown, D.B. & Burkalter, P.G. (1985). *Appl. Opt.* **24**, 2536.
Tuite, M.F. (1964). *Nature* **370**, 327.
Tuite, M.F. & Oliver, S.G. (1991). *Saccharomyces*. New York: Plenum Press.
Turcu, E., Ross, I., Trenda, P., Schulz, M., Michette, A.G., Tallents, G.J., Batani, D., Wharton, C.W., Meldrum, R.A., *et al*. (1994*a*). *SPIE Proc*. **2015**, 243.
Turcu, E., Tallents, G.J., Ross, I., Michette, A.G., Schulz, M., Meldrum, R.A., Wharton, C.W., Batani, D., Martinetti, M. & Mauri, A. (1994*b*). *Physica Medica* **10**, 93.
Warburg, O. (1930). *Metabolism of Tumor*. London: Arnold Constable Publishers.
Weast, R.C. & Astle, M.J. (1983). *Handbook of Chemistry and Physics*. Boca Raton, FL: CRC Press.
Winfree, A.T. (1983). *The Geometry of Biological Time*. Berlin: Springer-Verlag.

https://doi.org/10.1017/S0263034604223175 Published online by Cambridge University Press